AtBXL1 Encodes a Bifunctional β-D-Xylosidase/α-L-Arabinofuranosidase Required for Pectic Arabinan Modification in Arabidopsis Mucilage Secretory Cells[1][C][W][OA]

Andrej A. Arsovski, Theodore M. Popma, George W. Haughn, Nicholas C. Carpita, Maureen C. McCann, and Tamara L. Western*

Biology Department, McGill University, Montreal, Quebec, Canada H3A 1B1 (A.A.A., T.L.W.); Botany Department, University of British Columbia, Vancouver, British Columbia, Canada V6T 1Z4 (T.M.P., G.W.H.); and Department of Botany and Plant Pathology (N.C.C.) and Department of Biological Sciences (M.C.M.), Purdue University, West Lafayette, Indiana 47907

Following pollination, the epidermal cells of the Arabidopsis (*Arabidopsis thaliana*) ovule undergo a complex differentiation process that includes the synthesis and polar secretion of pectinaceous mucilage followed by the production of a secondary cell wall. Wetting of mature seeds leads to the rapid bursting of these mucilage secretory cells to release a hydrophilic gel that surrounds the seed and is believed to aid in seed hydration and germination. A novel mutant is identified where mucilage release is both patchy and slow and whose seeds display delayed germination. While developmental analysis of mutant seeds reveals no change in mucilage secretory cell morphology, changes in monosaccharide quantities are detected, suggesting the mucilage release defect results from altered mucilage composition. Plasmid rescue and cloning of the mutant locus revealed a T-DNA insertion in *AtBXL1*, which encodes a putative bifunctional β-D-xylosidase/α-L-arabinofuranosidase that has been implicated as a β-D-xylosidase acting during vascular development. Chemical and immunological analyses of mucilage extracted from *bxl1* mutant seeds and antibody staining of developing seed coats reveal an increase in (1→5)-linked arabinans, suggesting that BXL1 is acting as an α-L-arabinofuranosidase in the seed coat. This implication is supported by the ability to rescue mucilage release through treatment of *bxl1* seeds with exogenous α-L-arabinofuranosidases. Together, these results suggest that trimming of rhamnogalacturonan I arabinan side chains is required for correct mucilage release and reveal a new role for BXL1 as an α-L-arabinofuranosidase acting in seed coat development.

Differentiation of ovule integuments after pollination establishes a number of specialized cell types, including, in some species, the creation of a mucilaginous seed coat epidermis (myxospermy) (Esau, 1977; Fahn, 1982). Upon seed hydration, the epidermal cells of myxospermous seeds burst to release a hydrophilic, polysaccharide gel that has been suggested to play multiple roles, including promotion of seed hydration and prevention of desiccation during germination (Fahn, 1982). Mucilages are primarily composed of pectins, a complex, heterogeneous set of acidic polysaccharides that also compose the matrix of dicot primary cell walls (Fahn, 1979; Grubert, 1981; McCann and Roberts, 1991; Carpita and Gibeaut, 1993). The pectin rhamnogalacturonan I (RG I) is predominant in a number of seed mucilages (Naran et al., 2008) and is comprised of a backbone of alternating (1→2)-α-L-Rha and (1→4)-β-D-GalA. This backbone can be substituted with at least three different types of side chains on the Rha residues: arabinans, galactans, and type I arabinogalactans. Arabinans consist of (1→5)-α-L-Ara with occasional (1→3)- and (1→2)-α-L-Ara branch points, galactans are unbranched chains of (1→4)-β-D-Gal, and type I arabinogalactans are (1→4)-β-D-galactans that can be decorated with terminal Ara residues (Ridley et al., 2001; Willats et al., 2001a; Mohnen, 2008).

The Arabidopsis (*Arabidopsis thaliana*) seed coat mucilage secretory cells (MSCs) undergo a complex differentiation process, including mucilage synthesis and secondary cell wall production, that makes them an excellent model for understanding the developmental regulation of cell wall polysaccharide synthesis (Haughn and Chaudhury, 2005; Western, 2006). Following pollination, these cells undergo a phase of

[1] This work was supported by grants from the Natural Sciences and Engineering Research Council of Canada (T.L.W. and G.W.H.) and Grant DBI–0217552 from the National Science Foundation Plant Genome Research Program (N.C.C. and M.C.M.).

* Corresponding author; e-mail tamara.western@mcgill.ca.

The author responsible for distribution of materials integral to the findings presented in this article in accordance with the policy described in the Instructions for Authors (www.plantphysiol.org) is: Tamara L. Western (tamara.western@mcgill.ca).

[C] Some figures in this article are displayed in color online but in black and white in the print edition.

[W] The online version of this article contains Web-only data.

[OA] Open Access articles can be viewed online without a subscription.

www.plantphysiol.org/cgi/doi/10.1104/pp.109.138388

growth mediated by vacuolar expansion, which is succeeded by the biosynthesis and secretion of large quantities of pectinaceous mucilage to the upper tangential corners of the cell. This targeted secretion leads to the establishment of a volcano-shaped cytoplasm topped by a ring-shaped mucilage pocket, all subtending the primary cell wall. A secondary cell wall (columella) is then laid down interior to the mucilage pocket, filling in most of the cytoplasm, followed by cell death and desiccation (Beeckman et al., 2000; Western et al., 2000; Windsor et al., 2000; Young et al., 2008). Seed hydration leads to almost instantaneous mucilage release through the breakage of the outer primary cell wall and the formation of a gel capsule around the seed that has been demonstrated to aid germination (Western et al., 2000; Penfield et al., 2001). Staining of Arabidopsis mucilage has revealed the presence of two distinct layers: an outer, diffuse, water-soluble layer and an inner, dense layer that is strongly associated with the seed. Both layers have been demonstrated to be predominantly comprised of unbranched RG I, with smaller quantities of cellulose, homogalacturonan, arabinans, and galactans found in the inner adherent layer (Western et al., 2000, 2004; Penfield et al., 2001; Willats et al., 2001b; Macquet et al., 2007a; Naran et al., 2008; Young et al., 2008).

A number of genes required for mucilage production and MSC differentiation have been identified. These include the developmental regulator *APETALA2* (*AP2*), the epidermal cell differentiation factors *TRANSPARENT TESTA GLABRA1* (*TTG1*), *TTG2*, *TRANSPARENT TESTA2* (*TT2*), *TT8*, *ENHANCER OF GLABRA3*, *GLABRA2* (*GL2*), *MYB5*, and *MYB61*, all of which encode transcription factors and play roles in multiple developmental processes beyond seed coat differentiation (Koornneef, 1981; Jofuku et al., 1994; Rerie et al., 1994; Penfield et al., 2001; Johnson et al., 2002; Zhang et al., 2003; Gonzales et al., 2009; Li et al., 2009). A screen for mutants affected in mucilage extrusion led to the identification of the *MUCILAGE-MODIFIED* genes (*MUM1* to *MUM5*; Western et al., 2001). *mum4* mutants make a reduced amount of mucilage, *mum3* and *mum5* appear to be affected in mucilage composition, while *mum1* and *mum2* mutants are defective in mucilage release upon seed hydration. *MUM4* encodes a UDP-L-Rha synthase (RHAMNOSE SYNTHASE2 [RHM2]), an enzyme required for the synthesis of RG I, the primary pectin found in Arabidopsis seed mucilage (Usadel et al., 2004; Western et al., 2004; Oka et al., 2007). Analysis of *MUM4/RHM2* transcripts in mutants of the MSC-related transcription factors revealed that *MUM4* is specifically up-regulated by *GL2*, which works downstream of *TTG1* and *AP2* (Western et al., 2004). In contrast, *MUM2* encodes a β-galactosidase that modifies mucilage RG I side chains to allow correct hydration properties (Dean et al., 2007; Macquet et al., 2007b). Recently, a subtilisin-like Ser protease, AtSBT1.7, also was found to affect mucilage release, possibly through a role in the regulation of cell wall modification enzymes acting in MSCs (Rautengarten et al., 2008).

In this article, we describe a novel MSC mutant named *patchy* that demonstrates a slow and stochastic mucilage release. Our results reveal that *patchy* mutants are defective in the bifunctional β-D-xylosidase/α-L-arabinofuranosidase BXL1 and have an increased proportion of (1→5)-α-L-arabinan in both their extracted mucilage and seed coat cell walls. These data suggest that BXL1 acts as an α-L-arabinofuranosidase in differentiating MSCs, and such modification of the pectin structure is required for primary cell wall disruption and mucilage release.

RESULTS

patchy Mutants Exhibit Patchy and Delayed Mucilage Release

To identify genes required for the synthesis and extrusion of seed coat mucilage, pools of T-DNA insertion lines (Feldmann, 1991) were screened for the presence of mucilage when hydrated by staining with the pectin dye ruthenium red. With this treatment, wild-type seeds are surrounded by a thick, pink-staining capsule of mucilage (Fig. 1A). One novel mutant identified with this screen demonstrated a patchy mucilage release phenotype, in that mucilage release occurred only from random patches of seed coat epidermal cells, rather than from all cells as in wild-type seeds (Fig. 1, A versus B). Backcrosses revealed this phenotype is due to a mutation at a single locus (223 wild type: 84 mutant; $\chi^2 = 0.9131$; $P > 0.1$, degrees of freedom [df] = 1), which we named *PATCHY* to reflect the mucilage release phenotype.

To quantify more precisely the differences in extruded mucilage between wild-type and *patchy* mutants, the amount of mucilage release was determined. In analyzed samples of seeds, 88.0% to 95.7% of wild-type seeds were completely surrounded by mucilage, while only 2.7% to 17.3% of *patchy* seeds had complete mucilage envelopes (Table I). Furthermore, when a particular line was stained in ruthenium red without agitation and prehydration in water, it was found that the degree of mucilage release dropped sharply, suggesting that mechanical agitation can aid release for these mutants (Table I). Timing of mucilage release was determined by filming seed hydration in the presence of ruthenium red dye (Fig. 2). With wild-type seeds, bulging of cells is first seen within a few seconds, following which a diffuse cloudy layer forms around the seed that intensifies in staining over time. A second, denser layer of mucilage close to the seed becomes stained later (Fig. 2A; Western et al., 2000). Wild-type seeds consistently released their mucilage in under 1 min (n = 8 seeds, all of which released), while those *patchy* seeds that released any mucilage could take from 3.5 to 95 min, with an average release time of 26.3 min (SE = 5.6 min; n = 22 seeds that released out of 83 total seeds; Fig. 2B).

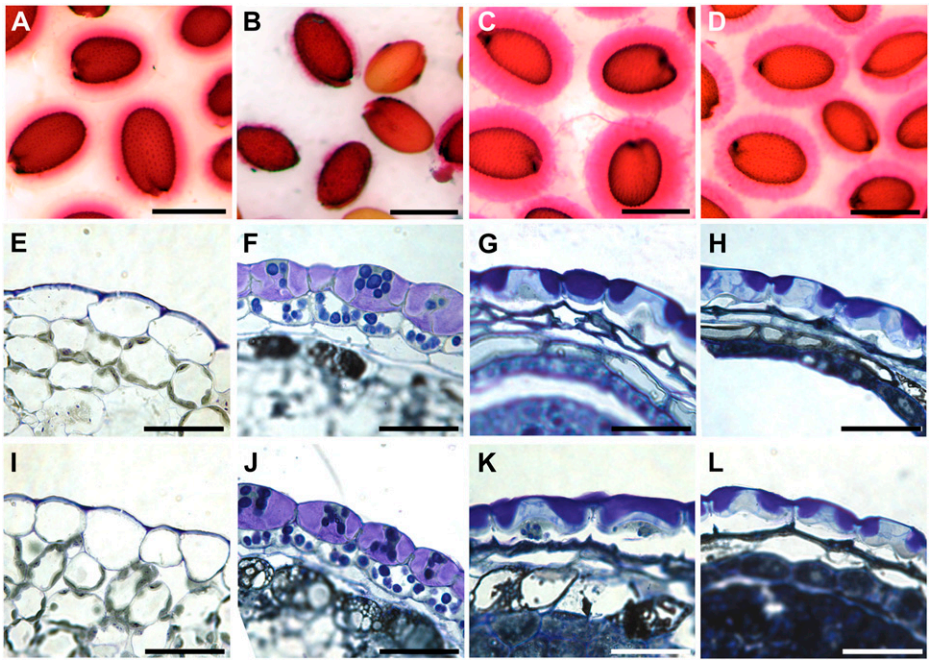

Figure 1. Ruthenium red staining and seed coat structure of *bxl1-1* versus wild-type Ws seeds. A and B, Wild-type (A) and *bxl1-1* (B) seeds shaken in water and then stained with ruthenium red. Note patchy mucilage staining around *bxl1-1* seeds. C and D, Wild-type (C) and *bxl1-1* (D) seeds stained with ruthenium red after shaking in 0.05 M EDTA. E to L, Cross sections of developing seed coat epidermal cells stained with toluidine blue. E to H, Wild type. E, 4 DPA with central vacuole filling most of cell. F, 7 DPA, purple-staining mucilage is accumulating. G, 10 DPA, dark purple-staining mucilage found in upper tangential regions of the cell, above the blue-staining secondary cell wall forming around the cytoplasm. H, 13 DPA, secondary cell wall (blue) has filled in the central region of the cell. I to L, *bxl1-1* mutant sections, note their similarity at each stage to the wild type. I, 4 DPA; J, 7 DPA; K, 10 DPA; L, 13 DPA. Bars = 200 μm in A to D and 50 μm in E to L.

patchy Mutants Appear to Undergo Normal Seed Coat Development But Have an Altered Mucilage Composition

Seeds making a severely reduced quantity of mucilage (e.g. *mum4/rhm2* mutants) demonstrate morphological changes at the cellular level as well as being defective in mucilage release (Western et al., 2001, 2004). Specifically, when observed with scanning electron microscopy, the columella found in the center of the MSCs is reduced in prominence in comparison to wild-type columellae (Supplemental Fig. S1, A versus B). This change in columella shape is accompanied by reduced intensity of mucilage staining with toluidine blue and smaller mucilage pockets. Sectioning and toluidine blue staining of developing *patchy* mutant seeds, however, shows similar mucilage staining, mucilage pocket size, and columella shape compared with the wild type (Fig. 1, E–L). This resemblance to the wild type is also observed when scanning electron microscopy is used to visualize the cell surface details (Supplemental Fig. S1, C versus D).

A threshold quantity of mucilage could be present in *patchy* mutants, making them look morphologically normal, but interfering with mucilage release in the stochastic manner observed. Alternately, mucilage hydration properties could be affected as in *mum2* mutants (Dean et al., 2007; Macquet et al., 2007b). Mucilage release can be induced in some reduced mucilage mutants by treatment with the heavy metal chelators, such as EDTA. Chelator treatment is believed to reduce binding of pectin chains through calcium bridges, allowing more extensive hydration and swelling of mucilage and/or weakening of the primary cell wall. When *patchy* seeds are treated with EDTA, and their mucilage levels compared to wild-type seeds, no gross difference was detected between the thickness of wild-type and *patchy* mucilage enveloping the seeds (compare Fig. 1, A and B with C and D).

To confirm this result, the mild chelator ammonium oxalate was used for extraction of mucilage, and the crude extracts were directly hydrolyzed and derivatized to alditol acetates (Table II). A slight but nonsignificant drop was observed both in the quantity of Rha and in total sugars. This was reflected in a small but significant decrease in both Fuc and Xyl. In addition, the amount of Ara increased approximately 1.5-fold (P value < 0.005) in *patchy* mucilage. Following mucilage extraction, the remaining seeds were also analyzed, but no significant differences in monosaccharide levels were observed (Table II). These results suggest that there is a change in mucilage composition that may be responsible for the slow and patchy mucilage release observed in the *patchy* mutants.

Table I. *Quantification of mucilage release of three independent lines of bxl1-1*

Seeds were shaken in water for 90 min followed by 60 min of shaking in 0.01% ruthenium red, except where noted. The proportion of an individual seed's circumference surrounded by mucilage was then quantified as 100% (seed completely surrounded by mucilage), 75% (3/4 of seed circumference surrounded), 50%, 25%, or no mucilage visible. Results are the percentage of seeds per sample with a particular mucilage category.

Line	Percentage of Seed Surrounded by Mucilage Capsule of Specified Size					
	100%	75%	50%	25%	No Mucilage	Total No. of Seeds
Ws #1	88.0	2.2	3.3	3.8	2.7	184
Ws #2	95.7	0	2.9	1.4	0	70
bxl1-1 line #1	2.7	6.1	43.5	38.8	8.8	147
bxl1-1 line #2	3.8	12.8	16.0	40.4	26.9	156
bxl1-1 line #3	17.3	21.0	29.6	21.6	10.5	162
bxl1-1 line #2[a]	3.6	0	7.2	15.7	73.5	83

[a]Seeds placed directly in ruthenium red with no pretreatment or shaking and monitored for 90 min (sample used for time lapse in Fig. 2).

patchy Seeds Show Delayed Germination in the Absence of Prehydration

General observation of growing *patchy* mutant plants revealed no significant vegetative differences compared to wild-type plants. A time course of seed germination revealed a 1- to 2-d delay of germination such that there is a roughly 40% reduction in germination in *patchy* mutants versus wild-type seeds at 3 d after plating, which becomes only 10% after 4 d (Fig. 3). However, prehydration of *patchy* seeds by shaking for 90 min in either water or EDTA restores germination to wild-type rates (Fig. 3). These data suggest that the changes in the mucilage of *patchy* mutants affect germination, presumably due to the reduced ability for *patchy* seeds to attract or hold water around the seed.

patchy Mutants Have Mutations in the Gene Encoding the Bifunctional β-D-Xylosidase/α-L-Arabinofuranosidase BXL1

The *patchy* mutant was isolated from a pool of T-DNA insertional mutants (CS2497; Feldmann, 1991). Kanamycin resistance encoded by the T-DNA was found to segregate with the mutant phenotype. In the F2 of a backcross to Wassilewskija (Ws), kanamycin-resistance segregated with a 3:1 ratio (161 resistant:62 sensitive; $\chi^2 = 0.9188$; $P > 0.1$, df = 1). Of the kanamycin-resistant plants, one-third had a patchy mucilage phenotype (115 wild type:48 patchy; $\chi^2 = 1.1203$; $P > 0.1$, df = 1), and 15 of these *patchy* mutants chosen at random gave rise to 100% kanamycin-resistant progeny. Southern-blot analysis with multiple T-DNA probes confirmed that the *patchy* mutant resulted from the insertion of a single, largely intact T-DNA of approximately 14 kb (data not shown). Using plasmid rescue, the insertion was located within the first intron of At5g49360, which encodes the putative β-D-xylosidase/α-L-arabinofuranosidase BXL1 (Goujon et al., 2003; Minic et al., 2004; Fig. 4A). Molecular complementation was performed using a genomic clone for At5g49360 under the endogenous promoter (PTYg; 8.1 kb of BAC K7J8, including 2.4 kb upstream and 1.2 kb downstream sequence). *patchy* mutants transformed with PTYg were found to have wild-type mucilage (9/10 independent transformants), while pGREEN0229-transformed plants retained the patchy mucilage phenotype (11/11) (Fig. 5, A and B; Supplemental Table S1). These results are consistent with the hypothesis that an insertion in *AtBXL1* is responsible for the seed coat phenotype.

Since the *patchy* mutant (renamed *bxl1-1*) has a T-DNA insertion in an intron (Fig. 4A), we examined the transcript level of *AtBXL1* in *bxl1-1* mutants using reverse transcription (RT)-PCR. In leaves, where *AtBXL1* is highly expressed, a strong band is found in wild-type Ws leaves, while a barely detectable band is seen for *bxl1-1* mutants at a saturating cycle number (Fig. 4B). Real-time PCR on 7 DPA seeds suggests that there is an approximately 1,000-fold decrease in transcript amount in *bxl1-1* mutants (Ws threshold cycle [C_t] = 21.8 ± 0.1 SE, $n = 3$; *bxl1-1* C_t = 32.1 ± 0.2 SE, $n = 3$). Two further T-DNA insertion lines in At5g49360 were obtained from the Salk Sequence Indexed Insertion collection (Alonso et al., 2003), which we named *bxl1-2* (Salk_012090) and *bxl1-3* (Salk_054483). *bxl1-2* has an insertion in exon 5, while the insertion in *bxl1-3* is in intron 5 (Fig. 4A). Both *bxl1-2* and *bxl1-3* have similar patchy mucilage release and germination phenotypes to *bxl1-1* and do not complement *bxl1-1* in genetic crosses, confirming they are insertions in the same gene (Supplemental Table S1; data not shown). Real-time PCR analyses reveal a decrease in the transcripts of both new alleles (22- and 450-fold for *bxl1-2* and *bxl1-3*, respectively; Columbia-0 [Col-0] C_t = 24.1 ± 0.4 SE; *bxl1-2* C_t = 28.6 ± 0.1 SE; *bxl1-3* C_t = 32.9 ± 0.4; $n = 3$). A truncation of the *bxl1-3* transcript beyond the insertion site was detected with RT-PCR. The *bxl1-2* transcript detected results from read-through of a large insertion (data not shown). Since the *bxl1-2* insertion

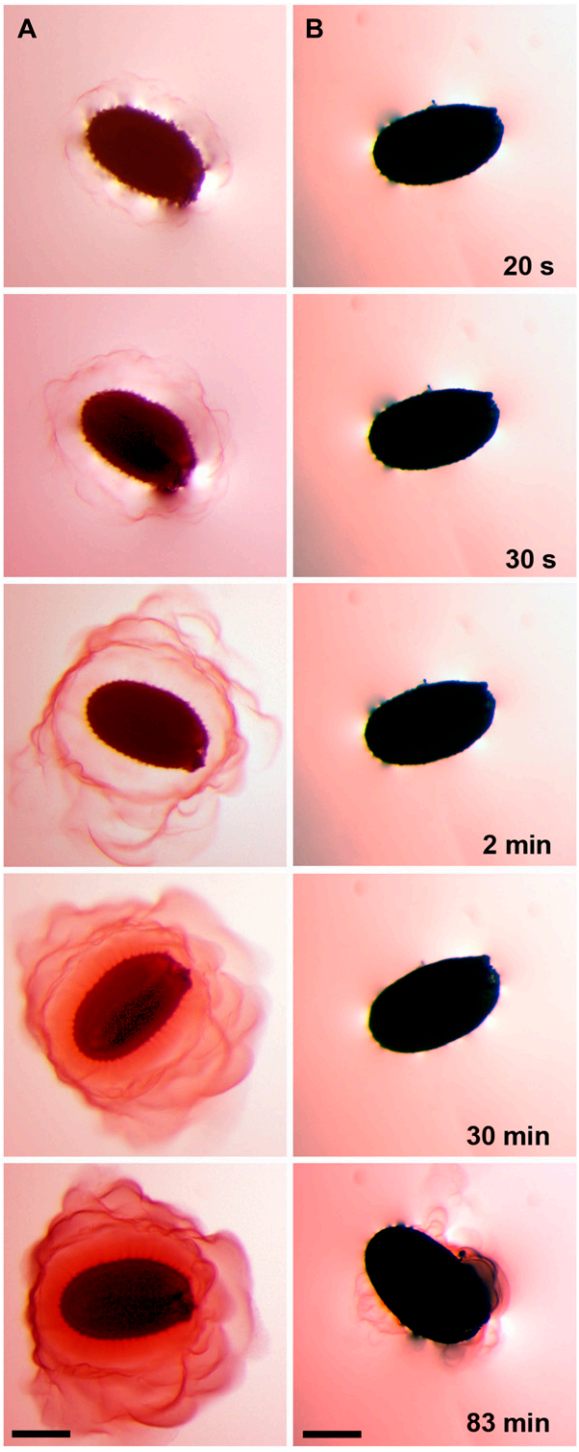

Figure 2. Time lapse of mucilage release for *bxl1-1* versus wild-type Ws seeds. Seeds were placed in ruthenium red solution and photographed over 90 min. A, Wild-type seed releases mucilage within 20 s and then mucilage stains pink over time. B, *bxl1-1* seed shows no mucilage release until 83 min, at which time mucilage is observed only for a patch of cells. Bars = 100 μm. [See online article for color version of this figure.]

lies upstream of the predicted catalytic Glu found in glycosyl hydrolase family three (GH3) enzymes (Minic et al., 2004), this insertion would be expected to render the protein nonfunctional. Because *bxl1-1* approaches a transcriptional null, all further analyses were performed on this allele.

AtBXL1 Is Transcribed throughout the Plant, Including in Differentiating Seed

RT-PCR was used for an initial determination of the transcription of *AtBXL1* throughout various tissues as well as in siliques before, during, and after the time of seed mucilage production (4, 7, and 10 DPA, respectively). *AtBXL1* transcripts were found in each of these tissues (Fig. 4B). Promoter-GUS experiments have shown that *AtBXL1* is expressed in the vasculature of the silique (Goujon et al., 2003); thus, we compared the transcription of *AtBXL1* in developing seeds versus siliques using real-time PCR (Fig. 4C). *AtBXL1* was found to be strongly expressed in both seeds and siliques at 7 and 10 DPA, with higher transcript levels (lower C_t) for siliques versus seeds. Separation of seeds from silique was not done for 4 DPA due to the difficulty of removing seeds at this stage.

bxl1 Mutants Have an Increase in the Proportion of Ara and Arabinan-Type Ara Linkages in Their Seed Coat Mucilage and Have Decreased α-L-Arabinofuranosidase Activity in Their Siliques

Since *AtBXL1* encodes a putative β-D-xylosidase/α-L-arabinofuranosidase, the mucilage composition was investigated more closely. Mucilage was sequentially extracted from seeds using the mild chelator ammonium oxalate, 0.2 and 2 N sodium hydroxide, to create fractions consisting of loosely attached pectins, more strongly linked pectins, and strongly linked pectins and cross-linking glycans (hemicelluloses), respectively. These extracts were extensively dialyzed to remove monosaccharide and chemical contaminants and analyzed for monosaccharide composition through carbodiimide activation and reduction with sodium borodeuteride followed by hydrolysis and derivatization to alditol acetates to allow for detection of both neutral sugars and uronic acids (Kim and Carpita, 1992; Carpita and McCann, 1996). For all three extracts, the primary sugars were Rha and GalA, reflecting isolation of mucilage that is largely composed of RG I (Table III; Penfield et al., 2001; Western et al., 2004; Naran et al., 2008). A decrease in the proportion of these two sugars, however, was seen in fractions from the harsher extractions, indicating the extraction of increased levels of RG I containing arabinan and galactan side chains as well as cellulose and other complex polysaccharides observed in the inner adherent layer of mucilage (Macquet et al., 2007a). Comparison between the extracts for the wild type and *bxl1-1* revealed increases in Ara in both ammonium oxalate and 0.2 N sodium hydroxide frac-

Table II. *Monosaccharide quantitation of bxl1-1 versus wild-type seeds*

Soluble polysaccharides from intact seeds were isolated by shaking in ammonium oxalate (soluble mucilage), followed by grinding of the same seeds and further ammonium oxalate extraction (seed minus soluble mucilage). Samples were then ethanol precipitated and directly hydrolyzed with trifluoroacetic acid followed by derivatization to alditol acetates. Results are given as average μg sugar per 100 mg seed and SE calculated from three independent samples.

Sugar	Soluble Mucilage		Seed Minus Soluble Mucilage	
	Ws	*bxl1-1*	Ws	*bxl1-1*
Rha	528 ± 23.6	486 ± 6.8	1,090 ± 85.7	937 ± 11.2
Fuc	5.1 ± 0.1	4.0 ± 0.1[a]	74.9 ± 2.4	72.8 ± 4.8
Ara	11.8 ± 0.7	17.5 ± 0.6[a]	1,610 ± 87.2	1,720 ± 8.5
Xyl	64.4 ± 2.7	53.7 ± 0.6[b]	578 ± 35.4	619 ± 4.7
Man	10.7 ± 0.6	10.4 ± 0.0	141 ± 9.9	137 ± 2.2
Gal	24.7 ± 1.9	25.1 ± 0.3	1,030 ± 60.0	985 ± 20.2
Glc	15.3 ± 1.7	13.8 ± 0.6	1,540 ± 129	1,370 ± 12.9
Total	660 ± 31.2	611 ± 8.6	6,050 ± 408	5,840 ± 50.3

[a]Significantly different from Ws, *P* value of <0.005. [b]Significantly different from Ws, *P* value of <0.05.

tions, with concurrent decreases in these same extracts for Xyl. The statistical significance of the ammonium oxalate Ara increase (*P* value = 0.002) is consistent with our earlier ammonium oxalate extracts without carboxyl reduction. Slight changes were also observed for Glc in 0.2 N sodium hydroxide (decrease), and Xyl, Glc (increase), Man, and Gal (decrease) in 2 N sodium hydroxide extracts.

To determine if more subtle changes in the chemical structure of the mucilage occur in *bxl1-1* extracts, analysis of the sugar linkages present was performed through per-*O*-methylation (Carpita and Shea, 1989; Gibeaut and Carpita, 1991) for all three extractions (Table IV). Similar to the monosaccharide analysis, few changes are observed between the wild type and *bxl1-1* across the extracts. The only difference that is consistently seen across all three extractions is an increase in the ratio of (1→5)-Ara (5-Ara*f*) in *bxl1-1* versus wild-type mucilage, which is consistent with the increased Ara at the monosaccharide level. Furthermore, the lack of change in the proportion of branch-point Rha residues (2,4-Rha*p*, 2,3-Rha*p*) suggests that the side chains of RG I are increased in size rather than abundance in the mutant. Several changes were observed in the 2 N sodium hydroxide extract: a decrease in both (1→2)-Rha (2-Rha*p*) and (1→4)-GalA (4-GalA*p*) suggests less RG I in the mutant. A slight change in xylan structure may also be occurring because in the 2 N sodium hydroxide extraction, there is a decrease in (1→4)-Xyl (4-Xyl*p*) accompanied by an increase in branch-point Xyl residues (2,4-Xyl*p*). The level of (1→4)-Man is also slightly decreased in this extraction. A similar slight change to branching of type II arabinogalactans is suggested in the 0.2 N sodium hydroxide extraction where there is a decrease in (1→6)-Gal and increase in branch-point Gal (3,6-Gal*p*).

To determine if there were any differences in cell wall composition beyond the mucilage, alcohol insoluble cell wall material was isolated from *bxl1-1* seedlings. Fourier transform infrared spectroscopy and monosaccharide analysis were performed. While the Fourier transform infrared results suggested the possibility of a slight change in pectin esterification (data not shown), no statistically significant differences were seen in the monosaccharide composition (Supplemental Table S2), consistent with the results of Goujon et al. (2003) for stems of antisense *BXL1* plants.

To confirm that the changes in Ara and arabinan levels found in extracted *bxl1-1* mucilage resulted from reduced α-L-arabinofuranosidase activity in *bxl1-1* mutants, enzyme assays were undertaken. Protein was extracted from developing wild-type and *bxl1-1* si-

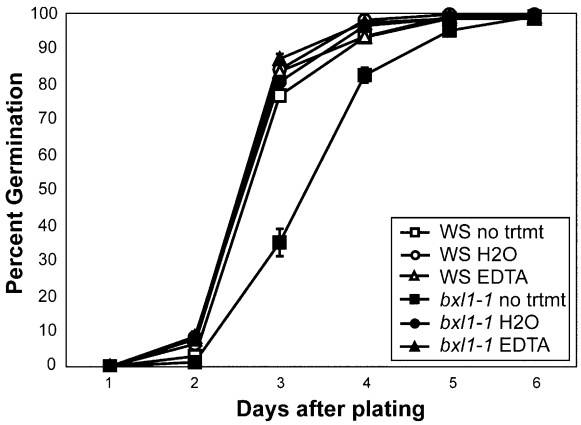

Figure 3. Germination of *bxl1-1* versus Ws (WS) wild-type seeds. Germination of seeds placed on minimal medium agar plates and cold treated for 72 h. Seeds were either plated directly as dry seeds (no trtmt) or prehydrated by shaking for 90 min in water (H2O) or 0.05 M EDTA as indicated, followed by suspension in 0.01% agarose and plating on minimal medium. Samples were done in triplicate with 50 to 60 seeds per sample. Error bars represent SE.

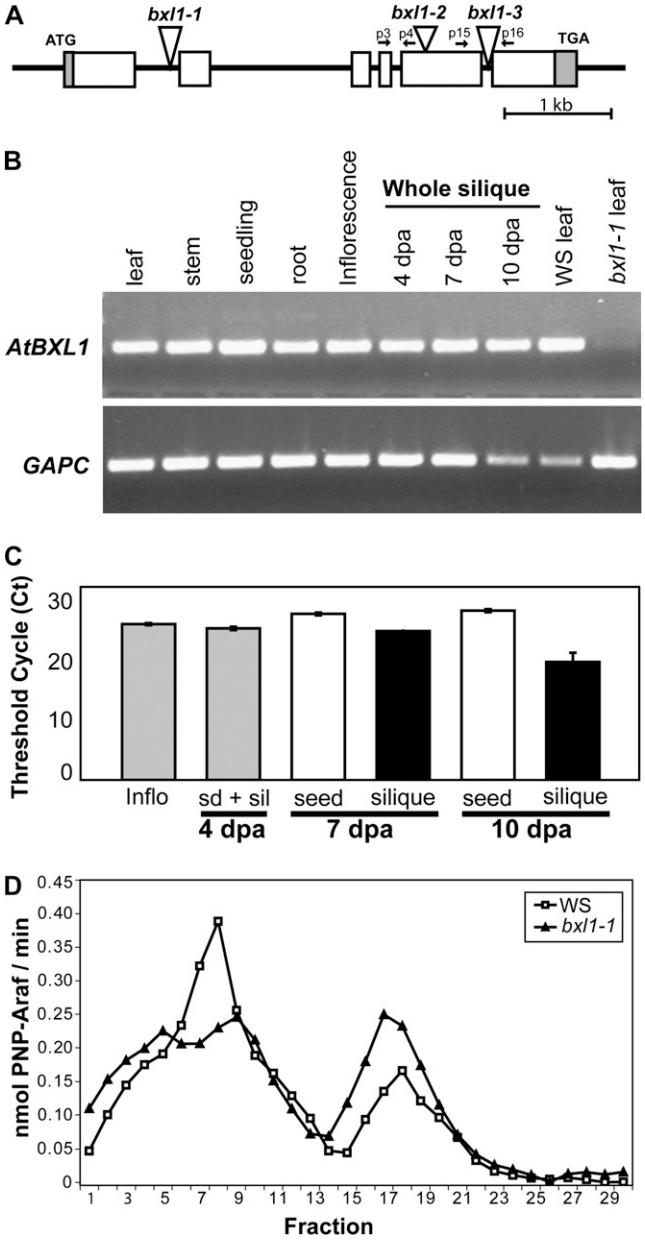

Figure 4. Structure and transcription of *AtBXL1*. A, Illustration of the intron-exon structure of *AtBXL1* showing the location of the different T-DNA insertions in *bxl1-1*, *bxl1-2*, and *bxl1-3*. Exons are drawn as boxes with gray shading indicating untranslated regions. T-DNA insertions are indicated by triangles. Locations of the primers used for the RT-PCR results shown in B and C are indicated with arrows. B, RT-PCR (30 cycles) using *AtBXL1* primers p15/16 on RNA isolated from Col wild-type leaves, stems, seedlings, roots, inflorescence tips, intact siliques at 4, 7, and 10 DPA, plus leaf tissue from wild-type Ws (WS) and *bxl1-1* plants. The loading control is cytosolic glyceraldehyde-3-P dehydrogenase (*GAPC*). C, Real-time PCR using *AtBXL1* primers p3/4 on inflorescences (inflo), intact 4-DPA siliques (sd + sil), and separated seeds and siliques at 7 and 10 DPA. Duplicate samples were performed using *GAPC* primers and used to normalize the *AtBXL1* results. Error bars represent SE, $n = 3$. D, Analysis of the α-L-arabinofuranosidase activity in *bxl1-1* mutant versus wild-type siliques using cation-exchange chromatography. Protein extracts were analyzed by SP-Sepharose chromatography and collected as 1-mL fractions. Each fraction was assayed for α-L-arabinofuranosidase activity and normalized against β-galactosidase activity from the same fraction.

liques, and fractions were collected after separation on a cation exchange column, following which α-L-arabinofuranosidase activity was assayed using *p*-nitrophenyl (PNP)-α-L-Ara*f*. Two peaks of α-L-arabinofuranosidase activity were detected, one of which was strongly reduced in the *bxl1-1* mutant, confirming that *bxl1-1* mutants have decreased α-L-arabinofuranosidase activity (Fig. 4D). An increase in the second peak was also observed in the *bxl1-1* mutant, suggesting possible compensation by one of the other two α-L-arabinofuranosidases identified in Arabidopsis siliques (Minic et al., 2006).

bxl1 Mutants Have an Increase in, and Altered Distribution of, RG I Arabinan Side Chains in Their Seed Coat Cell Walls

To confirm changes existed in the levels of (1→5)-linked arabinans in *bxl1-1* versus wild-type mucilage, immunoblots with extracted mucilage were performed using the arabinan-specific antibody LM6 (Willats et al., 1998, 2001b; Supplemental Fig. S2). The CCRC-M36 antibody specific to unbranched RG I and raised to Arabidopsis mucilage was used in parallel as a control (Young et al., 2008). Strong binding of LM6 was observed for EDTA extracts of *bxl1-1* mucilage, while staining was only faintly visible for wild-type samples (Supplemental Fig. S2A). Control immunoblots performed with CCRC-M36 showed roughly equal staining in the wild type and *bxl1-1*, suggesting a significant increase in (1→5)-linked arabinans in *bxl1-1* mucilage (Supplemental Fig. S2A).

Staining of developing seed coats with LM6 and CCRC-M36 was also performed. In wild-type seed coats, only faint staining was detected with LM6. The only significant staining of the MSCs was at the cell junctions on the lower face of the cells (Fig. 6A). By contrast, *bxl1-1* seed coats had very intense staining of all cell walls, including all cell walls of the MSCs (Fig. 6B), suggesting both a general increase in arabinans in *bxl1-1* seed coats and a specific increase in arabinans in the radial and outer cell walls of the MSCs. Similar to the immunoblot results, no significant differences were detected with CCRC-M36 staining (Fig. 6, C and D). Using whole seed immunofluorescence of mature seeds, the increase in cell wall LM6 staining was reflected in both the intensity of LM6 stain surrounding *bxl1-1* mutant seeds and the presence of clearly identifiable small sections of intact, hexagonal primary cell walls (Supplemental Fig. S2, D and E). These results suggest that the increase in LM6 epitopes within the wall may alter the mode of primary cell wall breakage during mucilage release in *bxl1* mutants.

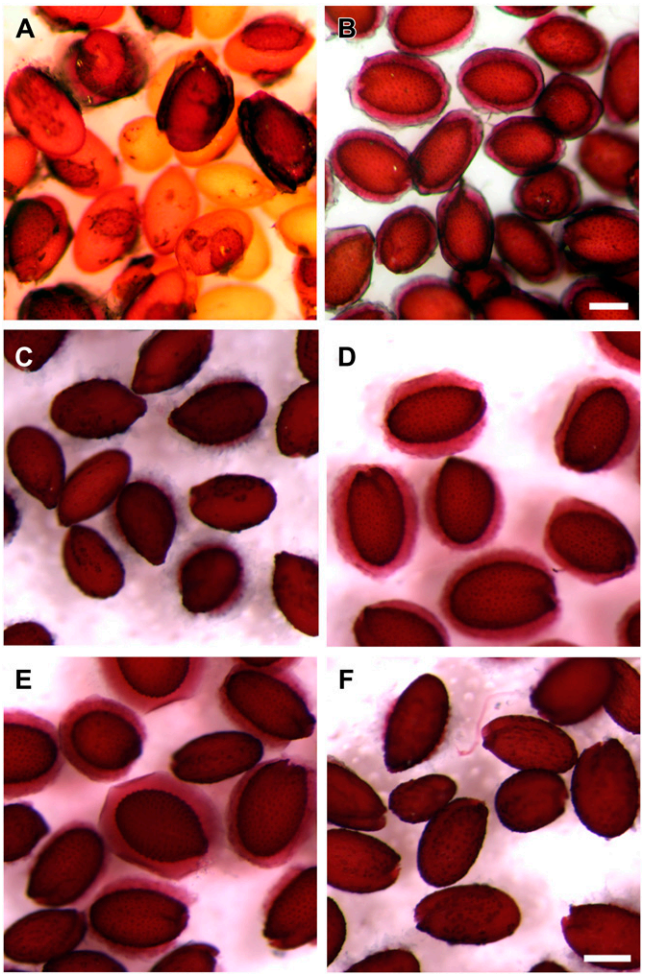

Figure 5. Molecular complementation with PTYg and phenotypic rescue of *bxl1-1* mutants with exogenous enzymes. A and B, Molecular complementation results demonstrating restoration of mucilage release in *bxl1-1* PTYg transformants (B) and patchy phenotype of *bxl1-1* pGREEN 0229-transformed control lines (A). C to F, Treatment of *bxl1-1* with exogenous enzymes. C, Enzyme buffer control; note patchy mucilage release. D and E, Treatment with α-L-arabinofuranosidases AN1571 (D) and AN7908 (E); note almost wild-type mucilage levels in (D) and significantly increased mucilage release in (E) compared to (C) and (F). F, Treatment with β-D-xylosidase AN2359; note patchy mucilage release. Bars = 200 μm.

The *bxl1* Mucilage Release Defect Can Be Rescued by Treatment with Exogenous α-L-Arabinofuranosidases

To test the potential role for an α-L-arabinofuranosidase in mucilage release, seeds were treated with recombinant enzymes obtained from an established collection of fungal polysaccharide degrading enzymes expressed in a secreted, affinity-tagged form in *Pichia pastoris* (Bauer et al., 2006). *bxl1-1* seeds were treated with three affinity-purified recombinant arabinofuranosidases (AN1571, AN7908, and AN80401; Bauer et al., 2006). Treatment with all three arabinofuranosidases led to rescue of the patchy mucilage release phenotype (Fig. 5, D and E), while treatment with enzyme buffer and a β-D-xylosidase (AN2359; Bauer et al., 2006) had no effect on mucilage release (Fig. 5, C and F). These rescue results suggest that removal of arabinans can promote mucilage release through modification of MSC walls and/or mucilage of *bxl1-1* mutants.

Genetic Interactions between *AtBXL1* and Known MSC-Related Transcription Factors

To test the genetic relationship between *AtBXL1* and known MSC genes, double mutant lines were constructed between *bxl1-1* and *ap2-1*, *ttg1-1*, *myb61-1*, and *mum4-1* mutants. The double mutants *bxl1-1 ap2-1* and *bxl1-1 ttg1-1* look identical to *ap2-1* (weak allele that shows reduced, patchy mucilage when EDTA treated) and *ttg1-1* (no mucilage release under EDTA treatment) mutants, respectively (Fig. 7, A–D). These results suggest an epistatic relationship, resulting either from regulation of *AtBXL1* by *AP2* and *TTG1* or a masking of the *bxl1* phenotype by the severity of the *ap2-1* and *ttg1-1* phenotypes. By contrast, *bxl1-1 myb61-1* double mutants have an additive phenotype in which the double mutant does not release mucilage when pretreated with water (Fig. 7, E versus F) but releases a similar amount to the *myb61-1* parent when treated with EDTA (data not shown). Thus, *AtBXL1* is acting independently from *MYB61* in the ability of seeds to release mucilage, suggesting that it is not regulated by *MYB61*. Unsurprisingly, *bxl1-1 mum4-1* double mutants also have an additive phenotype of no mucilage release when treated with EDTA (Fig. 7, G versus H), implying that the chelator-induced ability to release mucilage in mucilage-reduced *mum4* mutants is compromised by the loss of *AtBXL1* function. This enhancement of the *mum4-1* phenotype by *bxl1-1* suggests that the retention of mucilage release in the *ap2-1 bxl1-1* mutant, at least, may reflect true epistasis and possible regulation of *AtBXL1* by *AP2*.

Regulation of *AtBXL1* by AP2 and TTG1 was further investigated through real-time PCR of *AtBXL1* in 7-DPA seeds of *ap2-1* and *ttg-1* mutants, with only a slight but nonsignificant decrease in *AtBXL1* transcript being found in *ap2-1* mutants (data not shown).

DISCUSSION

Hydration of Arabidopsis seeds leads to the breakage of the outer primary cell wall of the MSCs and the release of pectinaceous mucilage to surround the seed (Western et al., 2000; Windsor et al., 2000). Our data reveal that the β-D-xylosidase/α-L-arabinofuranosidase BXL1 may play a role in mucilage release through the degradation of (1→5)-linked arabinans in the mucilage and/or primary cell wall. These results suggest a requirement for the trimming of RG I side chains to allow proper swelling of the mucilage and/or weakening of the primary cell wall to enable mu-

Table III. *Monosaccharide composition of mucilage extracted from bxl1-1 versus wild-type seeds*

Intact seeds were extracted sequentially with 0.2% ammonium oxalate, 0.2 N and 2 N NaOH, followed by carbodiimide reduction, trifluoroacetic acid hydrolysis, and alditol acetate derivatization. Results are given as average mole percentage and SE calculated from five independent samples.

Sugar	Ammonium Oxalate		0.2 N NaOH		2 N NaOH	
	Ws	*bxl1-1*	Ws	*bxl1-1*	Ws	*bxl1-1*
Rha	49.5 ± 0.4	49.7 ± 0.6	43.6 ± 2.4	44.2 ± 2.1	36.6 ± 1.8	37.1 ± 3.1
Fuc	tr[a]	tr	tr	tr	tr	tr
Ara	0.7 ± 0.1	1.3 ± 0.1[b]	2.6 ± 0.8	4.2 ± 0.7	9.3 ± 2.3	9.1 ± 1.0
Xyl	3.7 ± 0.2	3.3 ± 0.3	6.7 ± 2.0	5.5 ± 1.1	8.2 ± 2.4	9.4 ± 1.0
Man	1.0 ± 0.1	1.2 ± 0.1	2.2 ± 0.6	1.8 ± 0.3	3.2 ± 1.1	2.4 ± 0.9
Gal	1.8 ± 0.1	1.9 ± 0.1	2.9 ± 0.9	2.3 ± 0.3	5.1 ± 0.8	4.2 ± 0.7
Glc	2.3 ± 0.5	2.1 ± 0.3	4.8 ± 1.1	3.9 ± 1.1	9.4 ± 2.3	10.1 ± 6.3
GalA	40.9 ± 0.2	40.4 ± 0.5	37.2 ± 1.2	38.1 ± 1.2	28.2 ± 3.1	27.7 ± 3.3

[a]tr, Trace. [b]Significantly different from Ws, *P* value of 0.002.

cilage release. The requirement for developmentally coordinated changes to arabinan and RG I side chain numbers and branching is an emerging theme in the regulation of cell wall properties during plant growth and reproduction (Willats et al., 1999; Fulton and Cobbett, 2003; Lee et al., 2003, 2008; Leboeuf et al., 2004; Pena and Carpita, 2004; Tateishi et al., 2005; Minic et al., 2006; Xiong et al., 2007; Chávez Montes et al., 2008).

Mucilage Release Requires Modification of RG I Side Chains

bxl1 mutant slow and patchy mucilage release is correlated with a change in mucilage composition. These compositional changes appear to result in altered mucilage hydration properties, as water absorption tests of extracted mucilage suggest the speed of hydration and absorption capacity of *bxl1* mucilage are lower than those of wild-type mucilage (Supplemental Fig. S3). Chemical analysis and immunoblot results for *bxl1* mucilage revealed an increase in Ara and (1→5)-linked arabinans over wild-type mucilage (Tables III and IV; Supplemental Fig. S2), suggesting that chemical modifications to the mucilage in vivo may be required for sufficient mucilage swelling and release. The retention of a similar number of branchpoint 2,3- and 2,4-Rha*p* residues between *bxl1* and wild-type mucilage suggest that trimming of (1→5)-arabinans is occurring rather than the complete removal of the arabinan side chains from RG I polymers.

While chemical changes are observed in the extracted mucilage, a role for BXL1 in weakening of the outer primary cell wall to allow mucilage release is also supported. Mucilage release can be rescued through external treatment of *bxl1* seeds with exogenous α-L-arabinofuranosidases (Fig. 5, D and E), suggesting that more or larger arabinans are found in the primary cell wall in *bxl1* seeds. This is consistent with the intense staining of the cell walls of developing *bxl1* seeds hybridized with the arabinan-specific antibody LM6 (Fig. 6B; Willats et al., 1998). Failure to trim arabinans in the MSC primary cell wall may lead to wall stiffening in *bxl1* mutants, resulting in increased difficulty of cell wall breakage and the patchy mucilage release.

The exact contribution of increased cell wall strength versus reduced or slowed mucilage swelling to the altered cell wall breakage pattern seen in *bxl1* mutants is unclear. In wild-type MSCs, rapid pectin swelling is proposed to lead to rupture at the thin, radial cell walls and upward folding of the outer cell wall remnants still attached at the columella (Western et al., 2000; Windsor et al., 2000). In *bxl1* mutants, either slow-building pressure due to altered mucilage and/or prolonged pressure buildup resulting from a stronger primary cell wall could be expected to lead to outward bulging of the cell wall rather than immediate rupture. This continued bulging could eventually result in lifting of the whole surface cell wall upwards, breaking not only at the edges of the cell, but also severing connections to the columella, resulting in the hexagonal cell wall fragments observed in *bxl1* mutants (Supplemental Fig. S2).

Mucilage Release Requires the Activity of Multiple Genes

In addition to *AtBXL1*, several other genes have been demonstrated to play roles in mucilage release: *MUM1*, *MUM2*, and *AtSBT1.7* (Western et al., 2001; Dean et al., 2007; Rautengarten et al., 2008). While *MUM1* is yet to be cloned, the others appear to be involved, directly or indirectly, in structural modifications of the mucilage and/or outer cell wall that appear to be necessary for proper mucilage hydration and release. Similar to *AtBXL1*, *MUM2* encodes a glycosyl hydrolase, specifically a β-galactosidase, that is believed to be involved in the degradation of RG I side chains during MSC differentiation to allow the proper swelling and release of mucilage (Dean et al., 2007; Macquet et al., 2007b). *mum2* mucilage shows abnormally high levels of arabinans as well as terminal

Table IV. *Linkage analysis of extracted bxl1-1 versus wild-type mucilage*

Intact seeds were extracted sequentially with 0.2% ammonium oxalate, 0.2 and 2 N NaOH, followed by carbodiimide reduction. Linkage was then determined through per-*O*-methylation, trifluoroacetic acid hydrolysis, and alditol acetate derivatization. Results are given as the mean molar percentage ± variance of two samples, where 0 = <0.05.

Linkage	Ammonium Oxalate		0.2 N NaOH		2 N NaOH	
	Ws	*bxl1-1*	Ws	*bxl1-1*	Ws	*bxl1-1*
Fuc						
t-Fuc*p*	tr[a]	tr	tr	tr	tr	tr
Rha						
t-Rha*p*	0.4 ± 0	0.2 ± 0	0.5 ± 0.3	0.3 ± 0	0.3 ± 0.2	2.0 ± 5.5
2-Rha*p*	48.9 ± 0.6	48.6 ± 0.5	42.9 ± 0	42.5 ± 1.4	35.6 ± 3.7	24.5 ± 5.5
2,3-Rha*p*	0.4 ± 0.1	0.5 ± 0.2	0.4 ± 0.1	0.5 ± 0.5	0.4 ± 0.3	nd[b]
2,4-Rha*p*	1.0 ± 0.2	1.0 ± 0.1	1.4 ± 0	1.8 ± 0.5	0.7 ± 0.9	nd
Ara						
t-Ara*f*	0.1 ± 0	0.2 ± 0	1.2 ± 1.8	1.0 ± 0.6	1.8 ± 4.3	1.3 ± 1.8
2-Ara*f*	0.2 ± 0	0.3 ± 0	0.2 ± 0.1	0.1 ± 0	0.2 ± 0	0.2 ± 0.1
3-Ara*f*	tr	0.1 ± 0	1.3 ± 0	0.7 ± 0	0.2 ± 0.1	0.4 ± 0.3
5-Ara*f*	0.2 ± 0	0.9 ± 0	1.5 ± 0.1	2.4 ± 0.2	0.6 ± 0.7	3.0 ± 0.8
2,5-Ara*f*	tr	0.2 ± 0.1	1.0 ± 2.2	0.5 ± 0.5	0.7 ± 0.9	0.9 ± 1.8
3,5-Ara*f*	nd	0.1 ± 0	0.4 ± 0	0.5 ± 0	nd	nd
Xyl						
t-Xyl*p*	0.3 ± 0	0.2 ± 0	0.5 ± 0	0.2 ± 0	0.1 ± 0	0.1 ± 0
2-Xyl*p*	0.2 ± 0	0.2 ± 0	0.2 ± 0	0.2 ± 0	0.6 ± 0	0.4 ± 0
4-Xyl*p*	1.9 ± 0	1.6 ± 0	1.4 ± 0	1.6 ± 0	5.2 ± 0.7	3.7 ± 0.2
2,4-Xyl*p*	0.7 ± 0	0.6 ± 0	0.6 ± 0	0.5 ± 0	0.4 ± 0.3	1.2 ± 0.1
3,4-Xyl*p*	0.1 ± 0	0.1 ± 0	0.2 ± 0.1	tr	0.2 ± 0	tr
Man						
t-Man*p*	nd	nd	0.1 ± 0	0.1 ± 0	0.2 ± 0.1	0.2 ± 0
4-Man*p*	0.4 ± 0	0.5 ± 0	0.9 ± 0	1.0 ± 0	6.4 ± 0.5	4.6 ± 0
4,6-Man*p*	0.5 ± 0	0.4 ± 0	0.5 ± 0	0.4 ± 0	0.3 ± 0.2	0.6 ± 0
Gal						
t-Gal*p*	1.1 ± 0	0.9 ± 0	1.0 ± 0.3	0.6 ± 0	0.8 ± 1.4	0.9 ± 0
2-Gal*p*	nd	nd	0.3 ± 0.2	0.3 ± 0.2	nd	nd
3-Gal*p*	0.2 ± 0	0.3 ± 0	0.3 ± 0.1	0.1 ± 0	0.7 ± 1.0	1.6 ± 0.3
4-Gal*p*	0.1 ± 0	0.1 ± 0	0.1 ± 0	0.1 ± 0	4.1 ± 28.6	0.4 ± 0
6-Gal*p*	0.1 ± 0	0.1 ± 0	0.8 ± 0	0.5 ± 0	0.9 ± 1.8	nd
3,4-Gal*p*	0.1 ± 0	0.1 ± 0	0.2 ± 0	0.1 ± 0	0.1 ± 0	0.8 ± 1.4
3,6-Gal*p*	0.2 ± 0	0.5 ± 0	0.4 ± 0.4	1.8 ± 0	1.2 ± 2.7	2.8 ± 0.3
Glc						
t-Glc*p*	0.1 ± 0	0.1 ± 0	2.5 ± 2.1	3.2 ± 2.6	3.2 ± 1.0	15.5 ± 63.0
3-Glc*p*	nd	nd	nd	0.1 ± 0	0.1 ± 0	nd
4-Glc*p*	0.4 ± 0.3	0.8 ± 0	3.3 ± 0.8	3.4 ± 0.8	11.4 ± 0.2	14.8 ± 30.8
6-Glc*p*	nd	nd	0.2 ± 0.1	0.2 ± 0.0	0.6 ± 0.7	nd
2,4-Glc*p*	0.2 ± 0.1	0.1 ± 0	nd	nd	nd	nd
3,4-Glc*p*	tr	tr	0.4 ± 0	0.4 ± 0.1	0.5 ± 0.5	1.7 ± 1.4
4,6-Glc*p*	0.2 ± 0	0.1 ± 0	0.4 ± 0	0.5 ± 0	1.3 ± 0	2.1 ± 1.5
GalA						
t-GalA*p*	0.6 ± 0.1	0.5 ± 0	0.5 ± 0	0.5 ± 0	0.4 ± 0.2	0.8 ± 0.2
4-GalA*p*	39.3 ± 0.3	39.2 ± 0.2	32.4 ± 1.1	31.8 ± 0.9	19.7 ± 1.3	13.5 ± 0
3,4-GalA*p*	1.6 ± 0	1.6 ± 0.1	2.0 ± 0.9	1.8 ± 0.7	0.4 ± 0.4	0.4 ± 0.4
GlcA						
t-GlcA*p*	0.1 ± 0	0.2 ± 0	0.3 ± 0	0.5 ± 0	0.7 ± 0	0.9 ± 0

[a]tr, Trace. [b]nd, Not detected.

Gal residues and type 2 arabinogalactans (Dean et al., 2007; Macquet et al., 2007b), suggesting that MUM2 β-galactosidase activity may be required for activity of BXL1, possibly to allow access of BXL1 to its substrate. A requirement for the concerted activity of two or more glycosyl hydrolases for proper degradation of polysaccharides has been suggested previously for many enzymes, including other bifunctional β-D-xylosidases/α-L-arabinofuranosidases (Minic and Jouanin, 2006; Xiong et al., 2007; Minic, 2008).

Unlike the glycosyl hydrolases produced by *AtBXL1* and *MUM2*, the subtilisin-like Ser protease encoded by *AtSBT1.7* appears to work indirectly on primary cell wall and/or mucilage structure. *sbt1.7* mutants lack mucilage release when hydrated with water; however, treatment with EDTA leads to mu-

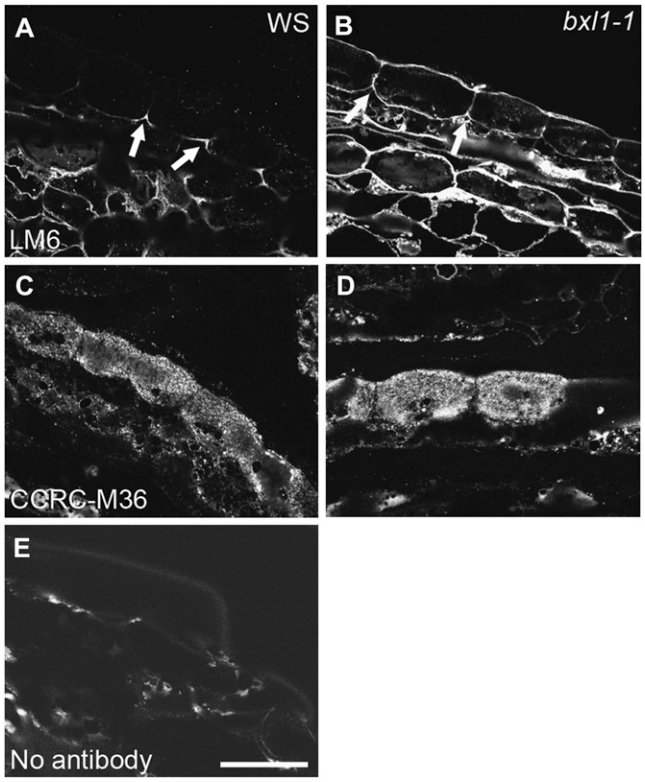

Figure 6. Immunofluorescence of developing Ws (WS) versus *bxl1-1* seeds coats. A and B, Confocal sections of 7-DPA Ws and *bxl1-1* seed coats stained with anti-arabinan antibody LM6. Arrows indicate lower corners of the mucilage cells; note intense staining around whole cell in *bxl1-1* mutants. C and D, Confocal sections of 7-DPA Ws and *bxl1-1* seed coats stained with unbranched RG I antibody CCRC-M36. E, Control image of Ws seed coat stained without primary antibody. Photo contrast was enhanced to visualize cells. All photographs were taken with the same microscope settings, save B, where the gain had to be reduced due to saturation of the image due to high intensity of fluorescence, making the image in B an underrepresentation of the degree of labeling. Bar = 50 μm.

cilage release and the shedding of a sheet of intact upper primary cell walls (Rautengarten et al., 2008). This latter phenotype is similar to, but more severe than, that seen in *bxl1* mutants and strongly points toward defects in the primary cell wall. However, as lack of mucilage release in *sbt1.7* mutants is associated with increased levels of demethylesterified mucilage and total seed cell walls, a role for altered mucilage behavior cannot be ruled out (Rautengarten et al., 2008). The identification of prolonged pectin methylesterase activity in *sbt1.7* mutants suggests both that AtSBT1.7 may inactivate these enzymes in vivo and that precise regulation of pectin methylesterase activity in developing MSCs is required (Rautengarten et al., 2008).

MSC differentiation, at least at the level of mucilage synthesis, appears to be regulated by a hierarchy of transcriptional regulators, as demonstrated by the specific up-regulation of the Rha synthase gene *MUM4/RHM2* by AP2 and TTG1 via GL2 (Western et al., 2004). Double mutant analysis revealed epistasis of *AP2* over *AtBXL1* and the possibility of similar regulation of *AtBXL1* by AP2 (Fig. 7). This correlates with a slight decrease in *AtBXL1* transcript levels in 7-DPA seeds with real-time PCR but should be further investigated through more specific analyses.

BXL1 Acts as a Bifunctional β-D-Xylosidase/α-L-Arabinofuranosidase in Vivo and Plays Different Roles in Different Tissues

AtBXL1 was identified by Goujon et al. (2003) as a gene encoding a β-xylosidase expressed in the vasculature, for which antisense plants with reduced β-xylosidase activity were found to have various growth defects, including short siliques and curled leaf edges. Our identification of an insertional mutant in *AtBXL1* with significantly reduced transcript, however, revealed only the patchy release of seed coat mucilage and delayed germination. The lack of a reported mucilage defect for the antisense lines may be due either to the patchy nature of the phenotype or the poor expression of the 35S promoter in MSCs (Young et al., 2008). The difference in whole plant phenotypes between *bxl1* and the *AtBXL1* antisense lines may be due to the additional knockdown of *AtBXL2* in the antisense plants. *AtBXL2* is 70% identical to *AtBXL1* at the nucleotide level, and its knockdown could not be ruled out by Goujon et al. (2003) using northern blots. RT-PCR of *AtBXL2* reveals that it has a lower, but overlapping, transcription pattern in most tissues where *AtBXL1* is expressed (leaves, stems, seedlings, roots, inflorescences, and 4-DPA siliques; Supplemental Fig. S4), and BXL2 has been copurified from stems with BXL1 in a proteomic analysis (Minic et al., 2007). Preliminary results suggest that *bxl1 bxl2* double mutants have shortened siliques and curled leaf edges similar to that observed in the antisense lines (data not shown).

While Goujon et al. (2003) suggested that BXL1 was functioning as a β-D-xylosidase in the stems, our chemical, enzymatic, and immunological analyses of *bxl1-1* mucilage and seed coat suggest that it is working as an α-L-arabinofuranosidase in seed MSCs due to the accumulation of both Ara and arabinans in *bxl1* mutants. The α-L-arabinofuranosidase function correlates with the data of Minic et al. (2004), who isolated BXL1 enzyme (XYL1) from Arabidopsis stems and demonstrated its activity as a bifunctional β-D-xylosidase/α-L-arabinofuranosidase with a substrate preference for sugar beet (*Beta vulgaris*) (1→5)-linked arabinan in in vitro enzyme assays. Taking both our data and those of Goujon et al. (2003), it appears that BXL1 performs two roles: that of a β-D-xylosidase and/or a bifunctional β-xylosidase/α-L-arabinofuranosidase in the remodeling of xylans in vascular development and that of an α-L-arabinofuranosidase in the cell wall of MSCs. BXL1 belongs to GH3, from which a number of enzymes have been characterized

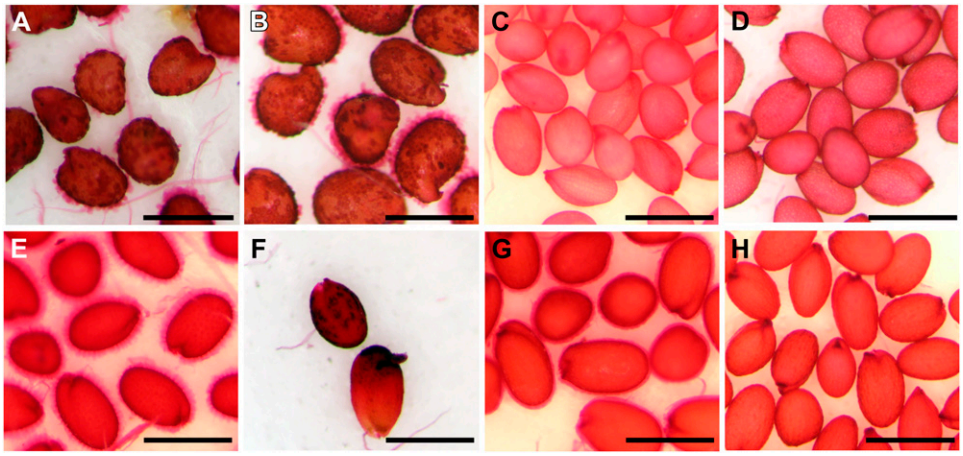

Figure 7. Phenotype of *bxl1-1* double mutants with *ap2-1*, *ttg1-1*, *myb61-1*, and *mum4-1*. Ruthenium red staining of single mutants and double mutants with *bxl1-1*, all shaken in 0.05 M EDTA to promote release of their small amount of mucilage prior to staining, except *myb61-1* and *bxl1-1 myb61-1* (E and F), which were shaken in water since *myb61-1* releases mucilage in water. A and B, *ap2-1* and *bxl1-1 ap2-1*, respectively. C and D, *ttg1-1* and *bxl1-1 ttg1-1*, respectively. E and F, *myb61-1* and *bxl1-1 myb61-1*, respectively; note mucilage release in *myb61-1* but not in the double mutant. G and H, *mum4-1* and *bxl1-1 mum4-1*, respectively; note thin layer of mucilage surrounding *mum4-1* seeds that is not seen in the double mutant. Bars = 500 μm.

to have β-xylosidase (XYL4/[At]BXL4), α-L-arabinofuranosidase ([At]BXL3, PpARF2, and [Hv]ARA-I), or bifunctional β-xylosidase/α-L-arabinofuranosidase activities (MsXyl1, [Hv]XYL, and RsAraf1; Lee et al., 2003; Minic et al., 2004, 2006; Tateishi et al., 2005; Kotake et al., 2006; Xiong et al., 2007). The bifunctional enzymes tend to have a substrate preference for arabinans in vitro and to be expressed in developing tissues, suggesting roles in the modification of primary cell walls rather than acting on secondary cell wall xylans (Kotake et al., 2006; Xiong et al., 2007). The bifunctionality of these enzymes has been suggested to allow flexibility of cell wall modifications with a limited number of enzymes. The activity of BXL1 as a β-xylosidase in stems (Goujon et al., 2003) and as an α-L-arabinofuranosidase in MSCs is the first in vivo demonstration of a bifunctional cell wall enzyme playing different roles in different tissues.

Regulation of RG I and Arabinan Side Chain Structure in Plant Growth and Development

Cell walls are heterogeneous and dynamic structures that vary in composition throughout growth and development (Carpita and Gibeaut, 1993; Somerville et al., 2004; Farrokhi et al., 2006). Arabinan and galactan side chains show developmental, tissue, cell type, and within-cell wall specificity in their localization (Willats et al., 1999, 2001a; McCartney et al., 2000; Orfila et al., 2001; Ridley et al., 2001; McCartney and Knox, 2002; Verhertbruggen et al., 2009). Roles for arabinans and their modification during development have come from the localization of arabinan epitopes to meristematic and proliferating root cells in carrots (*Daucus carota*) as well as the transcript expression pattern of both GH3 and GH51 α-L-arabinofuranosidases and bifunctional β-D-xylosidase/α-L-arabinofuranosidases in developing roots and stems (Willats et al., 1999; Fulton and Cobbett, 2003; Lee et al., 2003; Minic et al., 2006; Xiong et al., 2007; Chávez Montes et al., 2008). Modification of arabinan side chains, particularly debranching or trimming by α-L-arabinofuranosidases, also has been suggested in fruit ripening of Japanese pear (*Pyrus serotina*; Tateishi et al., 2005), storage of apples (*Malus domestica*; Pena and Carpita, 2004), pedicel abscission in poinsettia (*Euphorbia pulcherrima*; Lee et al., 2008), and in the growth of suspension-cultured microcalli (Leboeuf et al., 2004). These latter modifications have been correlated with loss of cell adhesion, while modulation of arabinan levels and branching during development may be associated with changes to cell wall elasticity as arabinans have been suggested to act as cell wall plasticizers and/or to form direct linkages between pectins and cellulose (Jones et al., 2003, 2005; Zykwinska et al., 2005, 2007; Moore et al., 2008).

The direct effects of a reduction in arabinan side chains have been observed both through the identification of Ara-deficient mutants in *Nicotiana plumbaginifolia* (*nolac-H14*) and Arabidopsis (*arad1*) and through ectopic expression of the family 51 α-L-arabinofuranosidase ARAF1 in Arabidopsis and a fungal endo-α-1,5-arabinanase in potato (*Solanum tuberosum*) tubers (Iwai et al., 2001; Skjøt et al., 2002; Harholt et al., 2006; Chávez Montes et al., 2008). While no obvious phenotypic effects were observed in Arabidopsis *arad1* mutants, *nolac-H14* mutants were identified through their reduced cell-cell adhesion, ARAF1 overexpression plants had delayed flowering time and altered stem architecture, and tissue from fungal arabinanase-expressing potatoes demonstrate altered wall stiffness (Iwai et al., 2001; Ulvskov et al., 2005; Harholt et al.,

2006; Chávez Montes et al., 2008). Our results complement and extend these data by demonstrating that the loss of arabinan modification in a specific cell type can lead to observable consequences on cell and plant developmental behavior: namely, the lack of cell wall breakage to facilitate mucilage release and consequent delayed seed hydration and germination.

MATERIALS AND METHODS

Plant Material and Growth Conditions

Lines of Arabidopsis (*Arabidopsis thaliana*) used were *bxl1-1* (Ws ecotype; CS16299), *bxl1-2*, *bxl1-3* (Salk_012090 [CS16300] and 054483 [CS16301], Arabidopsis Biological Resource Center [ABRC], Columbus, OH), *ap2-1*, *ttg1-1* (Landsberg *erecta* ecotype; ABRC), *myb61-1* (Col-0; gift from Michael Bevan, John Innes Centre, Norwich, UK), and *mum4-1* (Col-2; Western et al., 2004). Plants were grown and flowers staged as described by Western et al. (2001).

Microscopy

Developing seeds were staged and prepared for bright-field and scanning electron microscopy as described by Western et al. (2001). Ruthenium red staining was performed with 0.01% (w/v) ruthenium red with prehydration in either water or 0.05 M EDTA, as indicated.

Germination Tests

Seeds were either plated dry or pretreated by shaking for 90 min in water or 0.05 M EDTA and plated in 0.1% (w/v) agarose after rinsing. Seeds were stratified at 4°C for 72 h and incubated at 22°C under 16 h light:8 h dark, following which they were counted every day for 6 d and germination was scored by the presence of open green cotyledons.

Cloning of *AtBXL1* via Plasmid Rescue

Plasmid Rescue

DNA isolated from *patchy* mutants was digested with *Sal*I, *Eco*RI, or *Bgl*II, ligated, and transformed into *Escherichia coli*. Plasmid DNA isolated from the resulting colonies was sequenced to identify the genomic region flanking the T-DNA insertion using T-DNA right border and left border primers (Ponce et al., 1998).

Molecular Complementation

An 8.1 *Pml*I/*Pst*I fragment of BAC K7J8, including At5g49360 plus 2.4 kb upstream and 1.2 kb downstream sequences, was cloned into pGREEN0229 (Hellens et al., 2000) to give the PTYg construct. *patchy* plants were transformed with PTYg or the empty vector as in Clough and Bent (1998). Transformants were selected by germinating seeds on plates containing 25 μg/mL glufosinate, and putative transformants were verified by PCR.

Genetic Complementation

patchy mutants were crossed to Salk_012090 (*bxl1-2*) and Salk_054483 (*bxl1-3*), whose identities as At5g49360 mutants were verified through sequencing of the site of T-DNA insertion and use of RT-PCR to demonstrate reduced transcription and/or transcript truncation.

Qualitative and Real-Time RT-PCR

RNA was isolated as described by Western et al. (2004) or with a modified RNeasy plant mini protocol: two siliques were ground in liquid nitrogen, resuspended in 600 μL RLT-PVP40 (540 μL RLT + 60 μL 10% [w/v] polyvinylpyrrolidone) plus 10 μL β-mercaptoethanol per ml buffer and processed according to the manufacturer's instructions (Qiagen). One-microgram samples of total RNA were treated with DNaseI and transcribed with SuperScript II Reverse Transcriptase using an oligo(dT) primer according to the manufacturer's instructions (Invitrogen).

PCR for *AtBXL1* RT-PCR (Fig. 4B) was performed for 30 cycles using primers At5g49360 p 15/16, tests for truncated transcripts were performed with At5g49360 p 11/8, and *AtBXL2* RT-PCR was done with BXL2 p1/p2 (see Supplemental Table S3 for primer sequences). Real-time PCR was performed with an iCycler iQ Real-Time PCR system using the iQ SYBR Green Supermix (Bio-Rad). PCR conditions were 95°C for 10 min, 40 cycles of 30 s at 95°C, and 1 min at 55°C. Transcript levels were normalized against *GAPC*. Primers used were At5g49360 p3/p4 and RT-GAPCp5/p6.

Chemical Analyses

To quantify sugars in crude mucilage extracts, 50 mg of intact seeds were incubated in 0.2% (w/v) ammonium oxalate with vigorous shaking for 2 h at 30°C. No significant difference in mass was observed between Ws and *bxl1-1* seed (100 counted seed; Ws = 1.5 $\pm$ 0.1 mg; *bxl1* = 1.6 $\pm$ 0.0 mg; n = 3). One μmole of myo-inositol was added to the supernatant, and samples were precipitated with 5 volumes ethanol, directly hydrolyzed with 2 M trifluroacetic acid, and derivatized to alditol acetates (see below). For seedling cell walls, seedlings were dark treated for 48 h prior to harvest (150–200 mg of fresh weight), and alcohol-insoluble residues were prepared by grinding tissue in N_2 (l) plus 1% SDS (w/v), followed by extensive washing in alternating hot (80°C) water and 50% ethanol (60°C) with vacuum filtration.

For determination of monosaccharide ratios including GalA, five independent samples of 250 mg of seeds were extracted sequentially with 0.2% ammonium oxalate, 0.2 and 2 N sodium hydroxide, for 1 h each with vigorous shaking at 37°C. Both sodium hydroxide extractions contained 3 mg/mL sodium borohydride to prevent end degradation and were neutralized with acetic acid. The supernatants for each extraction were filtered through a glass fiber filter, dialyzed, and freeze dried. Carboxyl reduction was performed as described by Kim and Carpita (1992), as modified by Carpita and McCann (1996). Derivatization to alditol acetates was performed as described by Gibeaut and Carpita (1991). Linkage analysis through per-*O*-methylation was also performed as described by Gibeaut and Carpita (1991), with inferences on linkage structure as described by Carpita and Shea (1989).

Protein Isolation and Enzyme Assays

Preparation of Protein Extract

The 7-DPA Ws and *bxl1-1* siliques were ground in liquid nitrogen and extracted with 500 μL 25 mM MOPS, pH 7.0, and 0.5 mM Pefabloc and centrifuged for 10 min at 1,000*g*. The supernatant was collected and this constituted the soluble fraction. This was repeated three times and the fractions pooled. The remaining cell wall fraction was extracted with 2.5 mL 25 mM MOPS, pH 7.0, and 200 mM $CaCl_2$ during 1 h of vigorous shaking at 4°C. The tube was then centrifuged for 10 min at 1,000*g* and the supernatant (cell wall fraction) was recovered. The cell wall fraction was salt purified on a PD-10 column (GE Healthcare) according to the manufacturer's instructions.

Cation Exchange Chromatography

The cell wall fraction was equilibrated in 25 mM sodium acetate buffer (pH 5.0) containing 5% glycerol (v/v) and 0.015% Triton X-100 (v/v) and loaded on a HiTrap-FF SP-Sepharose column (GE Healthcare). The proteins were eluted with the same buffer, first alone and then with a 0.0 to 0.5 M NaCl continuous gradient. One-milliliter fractions were collected and 100 to 200 μL assayed from each fraction for α-L-arabinofuranosidase and β-D-galactosidase activity. Arabinofuranosidase activity was equalized to galactosidase activity in each fraction.

Enzyme Activity

The reaction mixture contained 2 mM PNP-α-L-arabinofuranose or PNP-β-D-galactopyranoside (Sigma-Aldrich), 0.1 M acetate buffer (pH 5.0), and 100 to 200 μL protein extract in a total volume of 0.5 mL. The reaction was carried out at 37°C for 90 min and stopped by the addition of 0.5 mL of 0.4 M sodium bicarbonate to the assay mixture. Concentration of the resulting PNP was determined spectrophotometrically at 405 nm, and its amount estimated from a calibration curve.

Immunoblotting and Immunofluorescence

For immunoblotting, 75 mg of seed were shaken in 0.05 M EDTA for 90 min at 37°C. Extracts were concentrated by evaporation and resuspended in 100 μL of PBS, pH 7.4, and 4 μL of concentrated mucilage spotted on nitrocellulose membranes as 2 × 2 μL aliquots. Hybridization was performed as described by Willats et al. (2001b) with the following modifications: membranes were blocked in antibody solution for 1 h, followed by incubation in primary antibody (1:10 [v/v] dilution of CCRC-M36 or LM6) for 90 min. Alkaline phosphatase-conjugated secondary antibodies (anti-mouse and anti-rat, respectively; Invitrogen) were diluted 1:1,000 (v/v) and detected using the BCIP/NBT-Purple liquid substrate (Sigma-Aldrich), with the reaction stopped by rinsing with water. CCRC-M36, an antibody specific for RG I, was obtained from CarboSource (University of Georgia, Athens; http://www.ccrc.uga.edu/~carbosource/CSS_home.html; Young et al., 2008), while LM6 is specific to (1→5)-linked arabinans (Willats et al., 1998) and was obtained from PlantProbes (University of Leeds, Leeds; http://www.plantprobes.net).

For immunofluorescence on developing seeds, seeds were dissected from 7- and 9-DPA siliques and fixed for 2 h in 4% (v/v) paraformaldehyde in 50 mM PIPES (pH 7.0). Samples were rinsed, dehydrated through an ethanol series, and embedded in LR White resin. Embedded samples were sectioned to 0.5 μm, affixed to slides with poly-L-Lys, and subjected to antibody detection as described by Young et al. (2008), except primary antibodies were used full strength and secondary antibodies were diluted as described below for whole seed samples. Whole seed immunofluorescence was performed as described by Young et al. (2008). Primary antibodies (1:20 [v/v]) were detected with a 1:100 (v/v) dilution of Alexfluor 488-conjugated goat anti-mouse (CCRC-M36) or goat anti-rat (LM6) secondary antibodies (Molecular Probes, Invitrogen). Seeds were counterstained with 0.2 μg/mL propidium iodide in 50 mM phosphate buffer, pH 7.4, to visualize the outer cell wall. Treatments without primary antibody were included to test for nonspecific staining, and all seeds were mounted in 1:100 (v/v) India ink in 90% (v/v) glycerol in water to confirm the presence of released mucilage. Immunofluorescence samples were observed with a Zeiss Meta 510 LSM confocal microscope.

Seed Treatment with Exogenous Enzymes

Pichia pastoris clones for three inducible, secreted, recombinant α-L-arabinofuranosidases (AN1571, AN7908, and AN80401), and one β-D-xylosidase (AN2359) were obtained from the Fungal Genetic Stock Center (www.fgsc.net; Bauer et al., 2006). Methanol treatment was used to induce secretion of recombinant enzymes into the medium. Cultures were then centrifuged and the enzymes were purified by affinity to their His tag from the supernatant as described by Bauer et al. (2005), with the exception that proteins were affinity isolated in a batch method (rather than in a column) using 1 mL of 50% Ni-NTA His Bind Slurry (EMD Biosciences) and 4 mL Ni-NTA Bind buffer (buffer A; EMD Biosciences). Protein quantitation and activity assays were carried out using PNP-glycosides as described above. For seed treatment, 10 units (defined as the amount of enzyme that would release 10 nM PNP/μg protein in 1 h) of each enzyme were used to treat seed in 800 μL of water for 90 min at 37°C. Seeds were then rinsed with water and stained with 0.01% ruthenium red with shaking for 60 min.

Water Absorption Measurements

A modified Bowmann capillary apparatus was set up as described by Cui (2001), using 2- to 3-mm glass tubing connecting a 1-mL serological pipet and a 15-mL sintered glass funnel. Water was added from the pipet end until it reached the sintered glass. Filter paper was placed on top of the sintered glass and allowed to equilibrate. Two to five milligrams of the dialyzed, freeze-dried mucilage fractions described above were placed on the saturated filter paper and the level of water in the pipet determined every 5 min for 30 min, followed by every 15 min up to 2 h.

Isolation of Double Mutants

F2 seeds were first screened for visual phenotypes (*ap2-1* heart shape seeds and *ttg1-1* yellow seeds) and/or aberrant of mucilage release in ruthenium red dye (*ap2-1*, *ttg1-1*, *myb61-1*, and *mum4-1*). Candidate plants were genotyped for the *bxl1-1* T-DNA insertion using PCR with At5g49360 p8/p11 (Supplemental Table S3) and T-DNA LB primer iPCR-LB (Ponce et al., 1998). Putative *bxl1-1 myb61-1* and *bxl1-1 mum4-1* double mutants, which lack non-seed coat phenotypes, had their *myb61-1* and *mum4-1* genotypes verified using PCR. The *myb61-1* dSPM insertion was confirmed using MYB61 p1/p2 and dSPM11 (Supplemental Table S3; Penfield et al., 2001). The *mum4-1* point mutation leads to the addition of a new *Mse*I site, which can be detected by digesting the PCR products from At1g53500 p1/p8 (Supplemental Table S3; Western et al., 2004).

Supplemental Data

The following materials are available in the online version of this article.

Supplemental Figure S1. Scanning electron microscopy of *bxl1-1* versus *mum4-1* and wild-type seed coat epidermal cells.

Supplemental Figure S2. Immunoblot of extracted mucilage and whole seed immunofluorescence of Ws versus *bxl1-1* seeds.

Supplemental Figure S3. Water absorption of *bxl1-1* versus wild-type mucilage extracts.

Supplemental Figure S4. Transcription of *AtBXL2* throughout Arabidopsis tissues and during seed and silique development.

Supplemental Table S1. Quantification of mucilage release of complemented lines of *bxl1-1*, plus *bxl1-2* and *bxl1-3*.

Supplemental Table S2. Monosaccharide quantitation of *bxl1-1* versus wild-type seedlings.

Supplemental Table S3. Primer sequences for RT-PCR, real-time PCR, and genotyping of double mutants.

ACKNOWLEDGMENTS

We thank Drs. Gillian Dean, Hugo Zheng, and Ms. Heather McFarlane for helpful discussions and comments on the manuscript. We are also grateful for the help of Tieling Zhang, Phoenix Bouchard-Kerr, Amin Osmani, and Kathryn Brown for their assistance in chemical analysis, isolation of double mutants, and RNA preparations and Dr. François Parcy for the modified RNeasy protocol suitable for seed and silique RNA.

Received March 10, 2009; accepted May 14, 2009; published May 20, 2009.

LITERATURE CITED

Alonso J, Stepanova AN, Leisse TJ, Kim CJ, Zimmerman J, Barajas P, Cheuk R, Gadrinab C, Heller C, Jeske A (2003) Genome-wide insertional mutagenesis of *Arabidopsis thaliana*. Science **301:** 653–657

Bauer S, Vasu P, Mort AJ, Somerville CR (2005) Cloning, expression, and characterization of an oligoxyloglucan reducing end-specific xyloglucanbiohydrolase from *Aspergillus nidulans*. Carbohydr Res **340:** 2590–2597

Bauer S, Vasu P, Persson S, Mort AJ, Somerville CR (2006) Development and application of a suite of polysaccharide-degrading enzymes for analyzing plant cell walls. Proc Natl Acad Sci USA **103:** 11417–11422

Beeckman T, De Rycke R, Viane R, Inzé D (2000) Histological study of seed coat development in *Arabidopsis thaliana*. J Plant Res **113:** 139–148

Carpita N, Gibeaut DM (1993) Structural models of primary cell walls in flowering plants: consistency of molecular structure with the physical properties of the walls during growth. Plant J **3:** 1–30

Carpita NC, McCann MC (1996) Some new methods to study plant polyuronic acids and their esters. *In* R Townsend, A Hotchkiss, eds, Progress in Glycobiology. Marcell Dekker, New York, pp 595–611

Carpita NC, Shea D (1989) Linkage structure of carbohydrates by gas chromatography-mass spectrometry of partially-methylated alditol acetates. *In* CJ Beirmann, GD McGinnis, eds, Analysis of Carbohydrates by GLC and MS. CRC Press, Boca Raton, FL, pp 155–216

Chávez Montes RA, Ranocha P, Martinez Y, Minic Z, Jouanin L, Marquis M, Saulnier L, Fulton LM, Cobbett CS, Bitton F, et al (2008) Cell wall modifications in Arabidopsis plants with altered α-L-arabinofuranosidase activity. Plant Physiol **147:** 63–77

Clough SJ, Bent AF (1998) Floral dip: a simplified method for Agro-

bacterium-mediated transformation of Arabidopsis thaliana. Plant J **46:** 735–743

Cui SW (2001) Polysaccharide Gums from Agricultural Products: Processing, Structures and Functionality. Technomic Publishing Company, Lancaster, PA

Dean GH, Zheng H, Tewari J, Huang J, Young DS, Hwang YT, Western TL, Carpita NC, McCann MC, Mansfield SD, et al (2007) The Arabidopsis *MUM2* gene encodes a β-galactosidase required for the production of seed coat mucilage with correct hydration properties. Plant Cell **19:** 4007–4021

Esau K (1977) Anatomy of Seed Plants, Ed 2. John Wiley & Sons, Toronto

Fahn A (1979) Secretory Tissues in Plants. Academic Press, San Francisco

Fahn A (1982) Plant Anatomy, Ed 3. Pergamon Press, Toronto

Farrokhi N, Burton RA, Brownfield L, Hrmova M, Wilson SM, Bacic A, Fincher GB (2006) Plant cell wall biosynthesis: genetic, biochemical and functional genomics approaches to the identification of key genes. Plant Biotechnol J **4:** 145–167

Feldmann KA (1991) T-DNA insertion mutagenesis in Arabidopsis: mutational spectrum. Plant J **1:** 71–82

Fulton LM, Cobbett CS (2003) Two α-L-arabinofuranosidase genes in *Arabidopsis thaliana* are differentially expressed during vegetative growth and flower development. J Exp Bot **54:** 2467–2477

Gibeaut DM, Carpita NC (1991) Tracing the biosynthesis of the cell wall in intact cells and plants. Selective turnover and alteration of cytoplasmic and cell wall polysaccharides of proso millet in liquid culture and *Zea mays* seedlings. Plant Physiol **97:** 551–561

Gonzales A, Mendenhall J, Huo Y, Lloyd A (2009) TTG1 complex MYBs, MYB5 and TT2, control outer seed coat differentiation. Dev Biol **325:** 412–421

Goujon T, Minic Z, El Amrani A, Lerouxel O, Aletti E, Lapierre C, Joseleau JP, Jouanin L (2003) *AtBXL1*, a novel higher plant (*Arabidopsis thaliana*) putative β-xylosidase gene, is involved in secondary cell wall metabolism and plant development. Plant J **33:** 677–690

Grubert M (1981) Mucilage or Gum in Seeds and Fruits of Angiosperms: A Review. Minerva Press, Munich

Harholt J, Jensen JK, Sørensen SO, Orfila C, Pauly M, Scheller HV (2006) ARABINAN DEFICIENT 1 is a putative arabinosyltransferase involved in biosynthesis of pectic arabinan in Arabidopsis. Plant Physiol **140:** 49–58

Haughn GW, Chaudhury A (2005) Genetic analysis of seed coat development in *Arabidopsis*. Trends Plant Sci **10:** 472–477

Hellens RP, Edwards EA, Leyland NR, Bean S, Mullineaux PM (2000) pGreen: a versatile and flexible binary Ti vector for *Agrobacterium*-mediated plant transformation. Plant Mol Biol **42:** 819–832

Iwai H, Ishii T, Satoh S (2001) Absence of arabinan in the side chains of the pectic polysaccharides strongly associated with cell walls of *Nicotiana plumbaginifolia* non-organogenic callus with loosely attached constituent cells. Planta **213:** 907–915

Jofuku KD, den Boer BGW, Montagu MV, Okamuro JK (1994) Control of Arabidopsis flower and seed development by the homeotic gene *APETALA2*. Plant Cell **6:** 1211–1225

Johnson CS, Kolevski B, Smyth DR (2002) *TRANSPARENT TESTA GLABRA2*, a trichome and seed coat development gene of Arabidopsis, encodes a WRKY transcription factor. Plant Cell **14:** 1359–1375

Jones L, Milne J, Ashford D, McQueen-Mason SJ (2003) Cell wall arabinan is essential for guard cell function. Proc Natl Acad Sci USA **100:** 11783–11788

Jones L, Milne JL, Ashford D, McCann MC, McQueen-Mason SJ (2005) A conserved functional role of pectic polymers in stomatal guard cells from a range of plant species. Planta **221:** 255–264

Kim JB, Carpita NC (1992) Changes in esterification of the uronic acid groups of cell wall polysaccharides during elongation of maize coleoptiles. Plant Physiol **98:** 646–653

Koornneef M (1981) The complex syndrome of *TTG* mutants. Arab Inf Serv **18:** 45–51

Kotake T, Tsuchiya K, Aohara T, Konishi T, Kaneko S, Igarashi K, Samejima M, Tsumuraya Y (2006) An α-L-arabinofuranosidase/β-D-xylosidase from immature seeds of radish (*Raphanus sativus* L.). J Exp Bot **57:** 2353–2362

Leboeuf E, Thoiron B, Lahaye M (2004) Physico-chemical characteristics of cell walls from *Arabidopsis thaliana* microcalli showing different adhesion strengths. J Exp Bot **55:** 2087–2097

Lee RC, Hrmova M, Burton RA, Lahnstein J, Fincher GB (2003) Bifunctional family 3 glycoside hydrolases from barley with α-L-arabinofuranosidase and α-D-xylosidase activity. Characterization, primary structures, and COOH-terminal processing. J Biol Chem **278:** 5377–5387

Lee Y, Derbyshire P, Knox JP, Hvoslef-Eide AK (2008) Sequential cell wall transformations in response to the induction of a pedicel abscission event in *Euphorbia pulcherrima* (poinsettia). Plant J **54:** 993–1003

Li SF, Milliken ON, Pham H, Seyit R, Napoli R, Preston J, Koltunow AM, Parish RW (2009) The *Arabidopsis* MYB5 transcription factor regulates mucilage synthesis, seed coat development, and trichome morphogenesis. Plant Cell **21:** 72–89

Macquet A, Ralet M-C, Kronenberger J, Marion-Poll A, North HM (2007a) *In situ*, chemical and macromolecular study of the composition of *Arabidopsis thaliana* seed coat mucilage. Plant Cell Physiol **48:** 984–999

Macquet A, Ralet MC, Oudet O, Kronenberger J, Mouille G, Marion-Poll A, North HM (2007b) A naturally occurring mutation in an *Arabidopsis* accession affects a β-D-galactosidase that increases the hydrophilic potential of rhamnogalacturonan I in seed mucilage. Plant Cell **19:** 3990–4006

McCann MC, Roberts K (1991) Architecture of the primary cell wall. *In* CW Lloyd, ed, Cytoskeletal Basis of Plant Growth and Form. Academic Press, New York, pp 109–129

McCartney L, Knox JP (2002) Regulation of pectic polysaccharide domains in relation to cell development and cell properties in the pea testa. J Exp Bot **53:** 707–713

McCartney L, Ormerod AP, Gidley MJ, Knox JP (2000) Temporal and spatial regulation of pectic (1-4)-β-D-galactan in cell walls of developing pea cotyledons: implications for mechanical properties. Plant J **22:** 105–113

Minic Z (2008) Physiological roles of plant glycoside hydrolases. Planta **227:** 723–740

Minic Z, Do CT, Rihouey C, Morin H, Lerouge P, Jouanin L (2006) Purification, functional characterization, cloning, and identification of mutants of a seed-specific arabinan hydrolase in *Arabidopsis*. J Exp Bot **57:** 2339–2351

Minic Z, Jamet E, Negroni L, der Garabedian PA, Zivy M, Jouanin L (2007) A sub-proteome of *Arabidopsis thaliana* mature stems trapped on Concanavalin A is enriched in cell wall glycoside hydrolases. J Exp Bot **58:** 2503–2512

Minic Z, Jouanin L (2006) Plant glycoside hydrolases involved in cell wall polysaccharide degradation. Plant Physiol Biochem **44:** 435–449

Minic Z, Rihouey C, Do CT, Lerouge P, Jouanin L (2004) Purification and characterization of enzymes exhibiting β-D-xylosidase activities in stem tissues of Arabidopsis. Plant Physiol **135:** 867–878

Mohnen D (2008) Pectin structure and biosynthesis. Curr Opin Plant Biol **11:** 266–277

Moore JP, Farrant JM, Driouich A (2008) A role for pectin-associated arabinans in maintaining the flexibility of the plant cell wall during water deficit stress. Plant Signal Behav **3:** 102–104

Naran R, Chen G, Carpita NC (2008) Novel rhamnogalacturonan I and arabinoxylan polysaccharides of flax seed mucilage. Plant Physiol **148:** 132–141

Oka T, Nemoto T, Jigami Y (2007) Functional analysis of *Arabidopsis thaliana* RHM2/MUM4, a multidomain protein involved in UDP-D-glucose to UDP-L-rhamnose conversion. J Biol Chem **282:** 5389–5403

Orfila C, Seymour GB, Willats WGT, Huxham IM, Jarvis MC, Dover CJ, Thompson AJ, Knox JP (2001) Altered middle lamella homogalacturonan and disrupted deposition of (1→5)-α-L-arabinan in the pericarp of *Cnr*, a ripening mutant of tomato. Plant Physiol **126:** 210–221

Pena MJ, Carpita NC (2004) Loss of highly branched arabinans and debranching of rhamnogalacturonan I accompany loss of firm texture and cell separation during prolonged storage of apple. Plant Physiol **135:** 1305–1313

Penfield S, Meissner RC, Shoue DA, Carpita NC, Bevan MW (2001) *MYB61* is required for mucilage deposition and extrusion in the *Arabidopsis* seed coat. Plant Cell **13:** 2777–2791

Ponce MR, Quesada V, Micol JL (1998) Rapid discrimination of sequences flanking and with T-DNA insertion in the Arabidopsis genome. Plant J **14:** 497–501

Rautengarten C, Usadel B, Neumetzler L, Hartmann J, Büssis D, Altmann T (2008) A subtilisin-like serine protease essential for mucilage release from Arabidopsis seed coats. Plant J **54:** 466–480

Rerie WG, Feldmann KA, Marks DM (1994) The *GLABRA2* gene encodes a

homeo domain protein required for normal trichome development in Arabidopsis. Genes Dev **8:** 1388–1399

Ridley BL, O'Neill MA, Mohnen D (2001) Pectins: structure, biosynthesis, and oligogalacturonide-related signaling. Phytochemistry **57:** 929–967

Skjøt M, Pauly M, Bush MS, Borkhardt B, McCann MC, Ulvskov P (2002) Direct interference with rhamnogalacturonan I biosynthesis in Golgi vesicles. Plant Physiol **129:** 95–102

Somerville CR, Bauer S, Brininstool G, Facette M, Hamann T, Milne J, Osborne E, Paredez A, Persson S, Raab T, et al (2004) Toward a systems approach to understanding plant cell walls. Science **306:** 2206–2211

Tateishi A, Mori H, Watari J, Nagashima K, Yamaki S, Inoue H (2005) Isolation, characterization, and cloning of α-L-arabinofuranosidase expressed during fruit ripening of japanese pear. Plant Physiol **138:** 1653–1664

Ulvskov P, Wium H, Bruce D, Jørgensen B, Qvist KB, Skjøt M, Hepworth D, Borkhardt B, Sørensen SO (2005) Biophysical consequences of remodeling the neutral side chains of rhamnogalacturonan I in tubers of transgenic potatoes. Planta **220:** 609–620

Usadel B, Kuchinsky AM, Rosso MG, Eckermann N, Pauly M (2004) *RHM2* is involved in mucilage pectin synthesis and is required for the development of the seed coat in Arabidopsis. Plant Physiol **134:** 286–295

Verhertbruggen Y, Marcus SE, Haeger A, Verhoef R, Schols HA, McCleary BV, McKee L, Gilbert HJ, Knox JP (April 20, 2009) Developmental complexity of arabinan polysaccharides and their processing in plant cell walls. Plant J http://dx.doi.org/10.1111/j.1365-313X.2009.03876.x

Western TL (2006) Changing spaces: the *Arabidopsis* mucilage secretory cells as a novel system to dissect cell wall production in differentiating cells. Can J Bot **84:** 622–630

Western TL, Burn J, Tan WL, Skinner DJ, Martin-McCaffrey L, Moffatt BA, Haughn GW (2001) Isolation and characterization of mutants defective in seed coat mucilage secretory cell development in Arabidopsis. Plant Physiol **127:** 998–1011

Western TL, Skinner DJ, Haughn GW (2000) Differentiation of mucilage secretory cells of the Arabidopsis seed coat. Plant Physiol **122:** 345–355

Western TL, Young DS, Dean GH, Tan WL, Samuels AL, Haughn GW (2004) *MUCILAGE-MODIFIED4* encodes a putative pectin biosynthetic enzyme developmentally regulated by *APETALA2*, *TRANSPARENT TESTA GLABRA1*, and *GLABRA2* in the Arabidopsis seed coat. Plant Physiol **134:** 296–306

Willats WGT, Marcus SE, Knox JP (1998) Generation of a monoclonal antibody specific to (1→5)-[α]-arabinan. Carbohydr Res **308:** 149–152

Willats WGT, McCartney L, Knox JP (2001b) In-situ analysis of pectic polysaccharides in seed mucilage and at the root surface of *Arabidopsis thaliana*. Planta **213:** 37–44

Willats WGT, McCartney L, Mackie W, Knox JP (2001a) Pectin: cell biology and prospects for functional analysis. Plant Mol Biol **47:** 9–27

Willats WGT, Steele-King CG, Marcus SE, Knox JP (1999) Side chains of pectic polysaccharides are regulated in relation to cell proliferation and cell differentiation. Plant J **20:** 619–628

Windsor JB, Symonds VV, Mendenhall J, Lloyd AL (2000) *Arabidopsis* seed coat development: morphological differentiation of the outer integument. Plant J **22:** 483–493

Xiong JS, Balland-Vanney M, Xie Z-P, Schultze M, Kondorosi A, Kondorosi E, Staehelin C (2007) Molecular cloning of a bifunctional β-xylosidase/α-L-arabinofuranosidase from alfalfa roots: heterologous expression in *Medicago truncatula* and substrate specificity of the purified enzyme. J Exp Bot **58:** 2799–2810

Young RE, McFarlane HE, Hahn MG, Western TL, Haughn GW, Samuels AL (2008) Analysis of the Golgi apparatus in *Arabidopsis* seed coat cells during polarized secretion of pectin-rich mucilage. Plant Cell **20:** 1623–1638

Zhang F, Gonzalez A, Zhao M, Payne CT, Lloyd A (2003) A network of redundant bHLH proteins function in all TTG1-dependent pathways. Development **130:** 4859–4869

Zykwinska AW, Ralet MCJ, Garnier CD, Thibault JFJ (2005) Evidence for in vitro binding of pectin side chains to cellulose. Plant Physiol **139:** 397–407

Zykwinska A, Thibault JF, Ralet MC (2007) Organization of pectic arabinan and galactan side chains in association with cellulose microfibrils in primary cell walls and related models envisaged. J Exp Bot **58:** 1795–1802